A Restricted Poincaré Map for Determining Exponentially Stable Periodic Orbits in Systems with Impulse Effects: Application to Bipedal Robots

B. Morris* and J.W. Grizzle*

***Abstract*— Systems with impulse effects form a special class of hybrid systems that consist of an ordinary, time-invariant differential equation (ODE), a co-dimension one switching surface, and a re-initialization rule. The exponential stability of a periodic orbit in a C^1-nonlinear system with impulse effects can be studied by linearizing the Poincaré return map around a fixed point and evaluating its eigenvalues. However, in feedback design—where one may be employing an iterative technique to *shape* the periodic orbit subject to it being exponentially stable—recomputing and re-linearizing the Poincaré return map at each iteration can be very cumbersome. For a nonlinear system with impulse effects that possesses an invariant hybrid subsystem and the transversal dynamics is sufficiently exponentially fast, it is shown that exponential stability of a periodic orbit can be determined on the basis of the restricted Poincaré map, that is, the Poincaré return map associated with the invariant subsystem. The result is illustrated on a walking gait for an underactuated planar bipedal robot.**

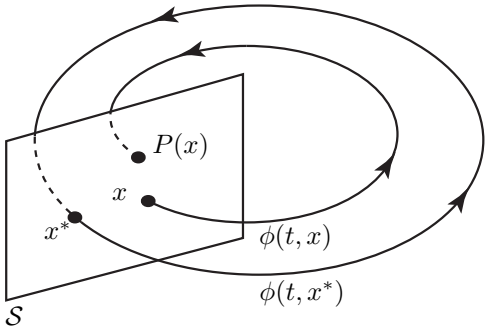

Fig. 1. Geometric interpretation of a Poincaré return map $P : \mathcal{S} \to \mathcal{S}$ for an ordinary differential equation (non-hybrid) as event-based sampling of the solution near a periodic orbit. The Poincaré section, $\mathcal{S}$, may be any co-dimension one (hyper) C^1-surface that is transversal to the periodic orbit.

I. Introduction

The method of Poincaré sections and return maps is widely used to determine the existence and stability of periodic orbits in a broad range of system models, such as time-invariant and periodically-time-varying ordinary differential equations [20], [13], hybrid systems consisting of several time-invariant ordinary differential equations linked by event-based switching mechanisms and re-initialization rules [11], [19], [22], differential-algebraic equations [14], and relay systems with hysteresis [9], to name just a few. While the analytical details may vary significantly from one class of models to another, on a conceptual level, the method of Poincaré is consistent and straightforward: sample the solution of a system according to an event-based or time-based rule, and then evaluate the stability properties of equilibrium points (also called fixed points) of the sampled system, which is called the Poincaré return map; see Fig. 1 and Fig. 2. Fixed points of the Poincaré map correspond[1] to *periodic orbits* of the underlying system. Roughly speaking, if the solutions of the underlying system depend continuously on the initial conditions, then equilibrium points of the Poincaré map are stable (asymptotically stable) if, and only if, the corresponding orbit is stable (asymptotically stable), and if the solutions are Lipschitz continuous in the initial conditions, then the equivalence extends to exponential stability.

The conceptual advantage of the method of Poincaré is that it reduces the study of periodic orbits to the study of equilibrium points, with the latter being a more extensively studied problem. The analytical challenge when applying the method of Poincaré lies in calculating the return map, which, for a typical system, is impossible to do in closed form because it requires the solution of a differential equation. Certainly, numerical schemes can be used to compute the return map, find its fixed points, and estimate eigenvalues for determining exponential stability. However, the numerical computations are usually time-intensive, and performing them iteratively as part of a system design process can be cumbersome. A more important drawback is that the numerical computations are not insightful, in the sense that it is very difficult[2] to establish a direct relationship between the parameters that a designer may be able to vary in a system and the existence or stability properties of a fixed point of the Poincaré map.

The objective of this paper is to augment the method of Poincaré with notions of invariance, attractivity, and time-scale separation in order to simplify its application to nonlinear systems with impulse effects, that is, systems modeled by an ordinary, time-invariant differential equation (ODE), a co-dimension one switching surface, and a re-initialization rule. Such models can be used to represent a wide range of systems with discontinuous or jump phenomena, including

* This work was supported by NSF grant ECS-0322395. B. Morris and J.W. Grizzle are with the Control Systems Laboratory, EECS Department, University of Michigan, Ann Arbor, Michigan 48109-2122, USA. E-mail: {morrisbj, grizzle}@umich.edu.

[1] Fixed points of $P^k = P \circ \cdots \circ P$ k-times also correspond to periodic orbits. The associated analysis problems for $k > 1$ are essentially the same as for $k = 1$ and are not discussed further.

[2] Of course, difficult does not mean impossible. There has been success with numerical implementations of Poincaré methods in the passive-robot community in terms of finding parameter values—masses, inertias, link lengths—for a given robot that yield asymptotically stable periodic orbits [10], [23], [18], [8].

walking and running gaits in legged robots. The experience gained in [24] has proven that when stability analysis can be rendered sufficiently simple, it becomes possible to efficiently explore a large set of asymptotically-stable gaits in order to find one that meets additional performance objectives, such as minimum energy consumption per distance traveled for a given average speed, or minimum peak-actuator power demand. The analytical results in [11] required that an invariant surface of the ODE portion of the model be rendered finite-time attractive through a continuous, but not Lipschitz continuous, feedback [3]. The result established in this paper will weaken this requirement to attractivity at a sufficiently-rapid exponential rate, thereby permitting the use of smooth feedback laws.

Section II provides background information on Poincaré's method for systems with impulse effects. Section III states conditions under which exponential stability of a periodic orbit in an invariant subsystem extends to exponential stability in the full system with impulse effects. The proof of this result is detailed in Section IV. The results of the paper are illustrated on a mathematical model of bipedal walking in Section V. A walking motion that was designed on the basis of a two-dimensional restriction dynamics is rendered exponentially stable in the full-order (ten-dimensional) model by use of a smooth feedback. A numerical investigation is performed to confirm the predictions of the theory. Conclusions are given in Section VI.

II. Background

This section reviews the method of Poincaré in the context of systems with impulse effects. The primary objective is to state a theorem linking the stability of fixed points of the Poincaré return map to the stability of periodic orbits of the underlying system.

A. Systems with impulse effects

An autonomous system with impulse effects consists of an autonomous ordinary differential equation,

$$\dot{x} = f(x), \tag{1}$$

defined on some state space $\mathcal{X}$, a co-dimension one surface $\mathcal{S} \subset \mathcal{X}$ at which solutions of the differential equation undergo a discrete transition that is modeled as an instantaneous re-initialization of the differential equation, and a rule $\Delta : S \to \mathcal{X}$ that specifies the new initial condition as a function of the point at which the solution impacts S [1], [25]. The system will be written as

$$\Sigma : \begin{cases} \dot{x} & = f(x) \quad x^- \notin \mathcal{S} \\ x^+ & = \Delta(x^-) \quad x^- \in \mathcal{S} \end{cases} \tag{2}$$

and said to be C^1 if the following conditions are satisfied:

H1.1) $\mathcal{X} \subset \mathbb{R}^N$ is open and connected,

H1.2) $f : \mathcal{X} \to \mathbb{R}^N$ is C^1

H1.3) $H : \mathcal{X} \to \mathbb{R}$ is C^1,

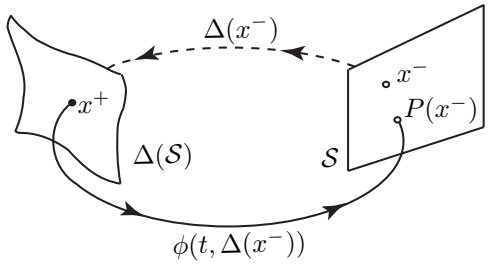

Fig. 2. Geometric interpretation of a Poincaré return map $P : \mathcal{S} \to \mathcal{S}$ for a system with impulse effects. The Poincaré section is selected as the switching surface, $\mathcal{S}$. A periodic orbit exists when $P(x^-) = x^-$. Due to right-continuity of the solutions, x^- is not an element of the orbit. With left-continuous solutions, $\Delta(x^-)$ would not be an element of the orbit.

H1.4) $\mathcal{S} := \{x \in \mathcal{X} \mid H(x) = 0\}$ is non-empty and $\forall x \in \mathcal{S}, \ \frac{\partial H}{\partial x}\big|_x \neq 0$ (that is, $\mathcal{S}$ is C^1 and has co-dimension one),

H1.5) $\Delta : \mathcal{S} \to \mathcal{X}$ is C^1, and

H1.6) $\Delta(\mathcal{S}) \cap \mathcal{S} = \emptyset$.

In simple terms, a solution of (2) is specified by the differential equation (1) until its state "impacts" the hyper surface $\mathcal{S}$ at some time t_I. At t_I, the impulse model Δ compresses the impact event into an instantaneous moment of time, resulting in a discontinuity in the state trajectory. The impact model provides the new initial condition from which the differential equation evolves until the next impact with $\mathcal{S}$. In order to avoid the state having to take on two values at the "impact time" t_I, the impact event is, roughly speaking, described in terms of the values of the state "just prior to impact" at time "t_I^-", and "just after impact" at time "t_I^+". These values are represented by x^- and x^+, respectively.

From this description, a formal definition of a solution is easily written down by piecing together appropriately initialized solutions of (1); see [25], [11], [19], [4]. A choice must be made whether to take a solution $\varphi(t)$ of (2) to be a left- or a right-continuous function of time at each impact event; here, solutions are assumed to be right continuous [11].

B. Periodic orbits

A solution $\varphi(t)$ of (2) is *periodic* if there exists a finite $T > 0$ such that $\varphi(t + T) = \varphi(t)$ for all $t \in [t_0, \infty)$. A set $\mathcal{O} \subset \mathcal{X}$ is a *periodic orbit* of (2) if $\mathcal{O} = \{\varphi(t) \mid t \geq t_0\}$ for some periodic solution $\varphi(t)$. While a system with impulse effects may certainly have periodic solutions that do not involve impact events, they are not of interest here because they could be studied more simply as solutions of (1). If a periodic solution has an impact event, then the corresponding periodic orbit $\mathcal{O}$ is not closed; see [11] and Fig. 2. Let $\bar{\mathcal{O}}$ denote its set closure.

Notions of stability in the sense of Lyapunov, asymptotic stability, and exponential stability of orbits follow the standard definitions; see [17, pp. 302], [11], [19]. For example, exponential stability is defined as follows. Given a norm $\|\cdot\|$ on $\mathcal{X}$, define the distance between a point x and a set $\mathcal{C}$ to be $\text{dist}(x, \mathcal{C}) := \inf_{y \in \mathcal{C}} \|x - y\|$. A periodic orbit $\mathcal{O}$ is

exponentially stable if there exists $\delta > 0$, $N > 0$ and $\gamma > 0$ such that, $\forall\ t \geq 0$,

$$\text{dist}(\varphi(t, x_0), \mathcal{O}) \leq Ne^{-\gamma t}\ \text{dist}(x_0, \mathcal{O}), \tag{3}$$

whenever $\text{dist}(x_0, \mathcal{O}) < \delta$.

Finally, a periodic orbit $\mathcal{O}$ is *transversal* to $\mathcal{S}$ if its closure intersects $\mathcal{S}$ in exactly one point, and for $\bar{x} := \bar{\mathcal{O}} \cap S$, $L_f H(\bar{x}) := \frac{\partial H}{\partial x}(\bar{x}) f(\bar{x}) \neq 0$ (in words, at the intersection, $\bar{\mathcal{O}}$ is not tangent to $\mathcal{S}$, where $\bar{\mathcal{O}}$ is the set closure of $\mathcal{O}$).

C. Poincaré return map

In the study of periodic orbits with impact events, it is natural to select $\mathcal{S}$ as the Poincaré section. To define the return map, let $\phi(t, x_0)$ denote the maximal solution of (1) with initial condition x_0 at time $t_0 = 0$. The *time-to-impact* function, $T_I : \mathcal{X} \to I\!R \cup \{\infty\}$, is defined by

$$T_I(x_0) := \begin{cases} \inf\{t \geq 0 | \phi(t, x_0) \in \mathcal{S}\} & \text{if } \exists\ t \text{ such that} \\ & \phi(t, x_0) \in \mathcal{S} \\ \infty & \text{otherwise.} \end{cases} \tag{4}$$

The Poincaré return map, $P : \mathcal{S} \to \mathcal{S}$, is then given as (the partial map)

$$P(x) := \phi(T_I \circ \Delta(x), \Delta(x)). \tag{5}$$

Theorem 1: Under hypotheses H1, if the system with impulse effects (2) has a periodic orbit $\mathcal{O}$ with $x^* := \bar{\mathcal{O}} \cap \mathcal{S}$ a singleton and $L_f H(x^*) \neq 0$, then the following are equivalent:

i) x^* is an exponentially stable (resp., asymp. stable, or stable i.s.L.) fixed point of P;

ii) $\mathcal{O}$ is an exponentially stable (resp., asymp. stable, or stable i.s.L.) periodic orbit.

Proof: The equivalences for stability in the sense of Lyapunov and asymptotic stability are proven in [11], [19]. The equivalence for exponential stability is proven here. Under hypotheses H1 and the transversality of the orbit, $T_I \circ \Delta$ is continuous in a neighborhood of x^* [11, App. B]. From H1.6, $T_I \circ \Delta(x^*) > 0$, and in combination with H1.2, it follows that there exists an open ball $\mathcal{B}_r(x^*),\ r > 0$, and numbers T_* and T^* such that for every $x_0 \in \mathcal{B}_r(x^*) \cap \mathcal{S}$, $0 < T_* \leq T_I \circ \Delta(x_0) \leq T^* < \infty$, and $\forall x \in \Delta(\mathcal{B}_r(x^*))$, a solution to (1) exists on $[0, T^*]$.

Assume that $\mathcal{O}$ is exponentially stable, as in (3). If necessary, shrink $\delta > 0$ such that $Ne^{-\gamma T_*}\delta < r$. Let $x_0 \in \mathcal{B}_\delta(x^*) \cap \mathcal{S}$ and define $x_{k+1} = P(x_k),\ k \geq 1$. Then, by induction, $\|x_k - x^*\| \leq Ne^{-kT_*\gamma}\text{dist}(x_0, \mathcal{O})$.

It is enough to show the converse for initial conditions in $\mathcal{S}$ near x^*. Assume that x^* is exponentially stable. Since exponential stability of x^* implies stability i.s.L., by [11], $\mathcal{O}$ is also stable i.s.L. Hence, there exists $\delta > 0$ such that $\text{dist}(x_0, \mathcal{O}) < \delta$ implies $\text{dist}(\varphi(t, x_0), \mathcal{O}) \leq r,\ t \geq 0$. Let $\mathcal{K} := \{x \in \mathcal{X} \mid \text{dist}(x, \mathcal{O}) \leq r\}$. Since $\mathcal{K}$ is compact and f and Δ are differentiable, there exists a constant $\bar{L} < \infty$ such that $\|f(x) - f(\bar{x})\| \leq \bar{L}\|x - \bar{x}\|$, for all $x, \bar{x} \in \mathcal{K}$, and $\|\Delta(x) - \Delta(\bar{x})\| \leq \bar{L}\|x - \bar{x}\|$, for all $x, \bar{x} \in \mathcal{K} \cap \mathcal{S}$. Let $L := \bar{L}e^{\bar{L}T^*}$. Then, using standard bounds for the Lipschitz dependence of the solution of (1) w.r.t. its initial condition [17, pp. 79], it follows that for $x \in \mathcal{B}_\delta(x^*) \cap \mathcal{S}$,

$$\begin{aligned} &\sup_{0 \leq t \leq T_I \circ \Delta(x)} \text{dist}(\phi(t, \Delta(x)), \mathcal{O}) \leq \\ &\sup_{0 \leq t \leq T^*} \|\phi(t, \Delta(x)) - \phi(t, \Delta(x^*))\| \leq \\ &\qquad L\|x - x^*\|. \end{aligned} \tag{6}$$

From this inequality, it follows easily that x^* being an exponentially stable fixed point of P implies the corresponding orbit is exponentially stable. ∎

Remark 1: Under the hypotheses of Theorem 1, P is differentiable at x^*. Indeed, the differentiability of T_I is proven in [20, App. D] at each point of $\tilde{\mathcal{S}} := \{x \in \mathcal{S} \mid T_I(x) < \infty \text{ and } L_f H(P(x)) \neq 0\}$. From this, the differentiability of Δ and f prove that P is differentiable on $\tilde{\mathcal{S}}$. Hence, exponential stability of orbits can be checked by linearizing P at x^* and computing eigenvalues.

III. Main Result

This section identifies a special structure for the system with impulse effects, (2), that will allow the exponential stability of periodic orbits to be determined on the basis of a restricted Poincaré map.

A. System structure

Consider a system with impulse effects that depends on a real parameter $\epsilon > 0$,

$$\Sigma^\epsilon : \begin{cases} \dot{x} = & f^\epsilon(x) & x^- \notin \mathcal{S} \\ x^+ = & \Delta(x^-) & x^- \in \mathcal{S}, \end{cases} \tag{7}$$

and suppose that for each value of $\epsilon > 0$, hypotheses H1 hold. For later use, a solution of $\dot{x} = f^\epsilon(x)$ is written as $\phi^\epsilon(t, x_0)$, the time-to-impact function is T_I^ϵ, and the Poincaré map is $P^\epsilon : \mathcal{S} \to \mathcal{S}$. In addition, suppose that the following structural hypotheses are met:

H2.1) there exist global coordinates $x = (z, \eta)$ for $\mathcal{X} \subset I\!R^n$, such that $z \in I\!R^k$, and $\eta \in I\!R^{n-k}$, $1 < k < n$, in which f^ϵ has the form

$$f^\epsilon(x) := f^\epsilon(z, \eta) := \begin{bmatrix} f_{1:k}(z, \eta) \\ f^\epsilon_{k+1:n}(\eta) \end{bmatrix};$$

H2.2) For $\mathcal{Z} := \{(z, \eta) \in \mathcal{X} \mid \eta = 0\}$, $\mathcal{S} \cap \mathcal{Z}$ is a $(k-1)$-dimensional, C^1-embedded submanifold of $\mathcal{Z}$, and

$$\Delta(\mathcal{S} \cap \mathcal{Z}) \subset \mathcal{Z}; \tag{8}$$

H2.3) (7) has a periodic orbit $\mathcal{O}$ that is contained in $\mathcal{Z}$, and hence the orbit is independent of ϵ;

H2.4) $x^* := \bar{\mathcal{O}} \cap \mathcal{S} \cap \mathcal{Z}$ is a singleton;

H2.5) $L_{f^\epsilon} H(x^*) \neq 0$;

H2.6) $f^\epsilon_{k+1:n}(\eta) = A(\epsilon)\eta$, and $\lim_{\epsilon \searrow 0} e^{A(\epsilon)} = 0$.

Hypotheses H2.1 and H2.6 imply that the set $\mathcal{Z}$ is invariant under the continuous part of the model, $\dot{x} = f^\epsilon(x)$, so that if $x_0 \in \mathcal{Z}$ then $\forall\ t$ in its maximal domain of existence, $\phi^\epsilon(t, x_0) \in \mathcal{Z}$. Hypothesis H2.2 implies that $\mathcal{Z}$ remains invariant across the impact event, and hence the solution of

(7) satisfies $x_0 \in \mathcal{Z}$ implies $\varphi(t, x_0) \in \mathcal{Z}$ on its domain of existence. Together, Hypotheses H2.1 and H2.2 imply that the restriction of Σ^ϵ to the manifold $\mathcal{Z}$ is a well-defined system with impulse effects, which will be called the *restriction dynamics*, $\Sigma_\mathcal{Z}$,

$$\Sigma_\mathcal{Z} : \begin{cases} \dot{z} = & f_\mathcal{Z}(z) & z^- \notin \mathcal{S} \cap \mathcal{Z} \\ z^+ = & \Delta_\mathcal{Z}(z^-) & z^- \in \mathcal{S} \cap \mathcal{Z} \end{cases}, \tag{9}$$

where $f_\mathcal{Z}(z) := f^\epsilon(z, 0)$, and $\Delta_\mathcal{Z} = \Delta(z, 0)$. Whenever convenient, z will also be viewed as an element of $\mathcal{X}$ by the identification $z = (z, 0)$. The invariance of $\mathcal{Z}$ also yields

$$P^\epsilon(\mathcal{S} \cap \mathcal{Z}) \subset \mathcal{S} \cap Z. \tag{10}$$

From Hypothesis H2.3, $\mathcal{O}$ is a periodic orbit of the restriction dynamics. The restriction of f^ϵ to $\mathcal{Z}$ removes any dependence on ϵ. This fact may be used to show that $\phi_\mathcal{Z} := \phi^\epsilon|_\mathcal{Z}$, $T_{I,\mathcal{Z}} := T_I|_\mathcal{Z}$, and $P^\epsilon|_\mathcal{Z}$ are also independent of ϵ, and hence,

$$t^* := T_I^\epsilon(\Delta(x^*)) \tag{11}$$

$$= T_{I,\mathcal{Z}}(\Delta_\mathcal{Z}(x^*)), \tag{12}$$

is independent of ϵ.

On the basis of (10), the *restricted Poincaré map*, $\rho : \mathcal{S} \cap \mathcal{Z} \to \mathcal{S} \cap \mathcal{Z}$, may be defined as $\rho := P^\epsilon|_\mathcal{Z}$, or equivalently,

$$\rho(z) := \phi_\mathcal{Z}(T_{I,\mathcal{Z}} \circ \Delta_\mathcal{Z}(z), \Delta_\mathcal{Z}(z)), \tag{13}$$

and is independent of ϵ. From H2.4, it follows that x^* is a fixed point of P^ϵ and ρ, and from H2.5, the orbit is transversal to $\mathcal{S}$, and hence also to $\mathcal{S} \cap \mathcal{Z}$.

Hypothesis H2.6 says that the dynamics transversal to $\mathcal{Z}$ is "strongly" exponentially contracting. When the solution of (7) is not on the periodic orbit, $\eta(t) \neq 0$. In many situations, such as bipedal walking, the impact map increases the norm of η at each impact; see Fig. 5. Hypothesis H2.6 provides control over the speed with which $\eta(t)$ converges to zero during the continuous phase, so that, over a cycle consisting of an impact event followed by continuous flow, the solution may converge to the orbit.

B. Main theorem

Theorem 2 (Main Theorem): Under Hypotheses H1 and H2, there exists $\bar{\epsilon} > 0$ such that for $0 < \epsilon < \bar{\epsilon}$, the following are equivalent:

i. x^* is an exponentially stable fixed point of ρ;
ii. x^* is an exponentially stable fixed point of P^ϵ.

□

In other words, for $\epsilon > 0$ sufficiently small, an exponentially stable periodic orbit of the restriction dynamics is also an exponentially stable periodic orbit of the full-order model.

IV. Proof of the Main Theorem

Throughout this section, Hypotheses H1 and H2 are assumed to hold. The proof is based upon evaluating $\mathcal{D}P^\epsilon(x^*)$, the linearization of the Poincaré map about the fixed point, in a set of local coordinates. This is a commonly employed technique even for system with impulse effects [10], [23], [18], [8]. The new result here will be an expression for $\mathcal{D}P^\epsilon(x^*)$ that brings out its structure due to Hypotheses H2.

A. Preliminaries

The usual approach to evaluating $\mathcal{D}P^\epsilon(x^*)$ is to view P^ϵ as a map from an open subset of $\mathbb{R}^n$ to $\mathbb{R}^n$. The linearization is then an $n \times n$ matrix and it must subsequently be shown that one of its eigenvalues is always one and the remaining $n-1$ eigenvalues are those of $\mathcal{D}P^\epsilon(x^*) : T_{x^*}\mathcal{S} \to T_{x^*}\mathcal{S}$; see [20], [14]. Here, local coordinates on $\mathcal{S}$ will be used so that $\mathcal{D}P^\epsilon(x^*)$ is computed directly as an $(n-1) \times (n-1)$ matrix.

In the coordinates $x = (z, \eta)$, H2.4 implies that $x^* = (z^*, 0)$. Since $f^\epsilon_{k+1:n}(0) = 0$, H2.5 is equivalent to $\frac{\partial H}{\partial z}(z^*, 0) f_{1:k}(z^*, 0) \neq 0$, which, writing $z = (z_1, \cdots, z_k)$, is equivalent to $\sum_{i=1}^k \frac{\partial H}{\partial z_i}(z^*, 0) f_i(z^*, 0) \neq 0$. If necessary, the components of z can always be re-ordered so that

$$\frac{\partial H}{\partial z_1}(z^*, 0) f_1(z^*, 0) \neq 0; \tag{14}$$

this will allow $(z_{2:k}, \eta)$, where $z_{2:k} = (z_2, \cdots, z_k)$, to be used as coordinates for $\mathcal{S}$. Indeed, (14) implies that $\frac{\partial H}{\partial z_1}(z^*, 0) \neq 0$, and hence by the Implicit Function Theorem, there exists a continuously differentiable scalar function Γ on an open neighborhood of x^* such that

$$(z_1, z_{2:k}, \eta) \in \mathcal{S} \Leftrightarrow z_1 = \Gamma(z_{2:k}, \eta).$$

It follows that

$$(z_1, z_{2:k}, \eta) \in \mathcal{S} \cap \mathcal{Z} \Leftrightarrow z_1 = \Gamma(z_{2:k}, 0) \text{ and } \eta = 0.$$

Letting $\hat{\Delta}$ be the representation of Δ in local coordinates on $\mathcal{S}$ gives

$$\hat{\Delta}(z_{2:k}, \eta) := \Delta(\Gamma(z_{2:k}, \eta), z_{2:k}, \eta). \tag{15}$$

Defining the projection π by

$$\pi(z_1, z_{2:k}, \eta) = (z_{2:k}, \eta), \tag{16}$$

then allows P^ϵ to be expressed in local coordinates $(z_{2:k}, \eta)$ on $\mathcal{S}$ by

$$\hat{P}^\epsilon(z_{2:k}, \eta) := \pi \circ \phi^\epsilon \left(T_I^\epsilon \circ \hat{\Delta}(z_{2:k}, \eta), \hat{\Delta}(z_{2:k}, \eta) \right). \tag{17}$$

Similarly, the restricted Poincaré map in local coordinates $z_{2:k}$ on $\mathcal{S} \cap \mathcal{Z}$ is given by

$$\hat{\rho}\left(z_{2:k}\right) := \pi_2 \circ \hat{P}^\epsilon \circ \mathcal{I}\left(z_{2:k}\right), \tag{18}$$

where

$$\pi_2(z_{2:k}, \eta) = z_{2:k}, \text{ and } \mathcal{I}\left(z_{2:k}\right) = (z_{2:k}, 0). \tag{19}$$

B. Application of the chain rule

The proof is broken down into three lemmas which together prove the Main Theorem. The first involves the *trajectory sensitivity matrix* of $\dot{x} = f^\epsilon(x)$, which is defined by[3]

$$\Phi^\epsilon(t, x_0) := \mathcal{D}_2\phi^\epsilon(t, x_0) \tag{20}$$

[3]For a differentiable function $g(x_1, x_2, ..., x_p)$, the notation $\mathcal{D}_i g(y_1, y_2, ..., y_p)$ refers to $\partial g/\partial x_i$ evaluated at $(x_1, x_2, ..., x_p) = (y_1, y_2, ..., y_p)$. The argument x_i may be a vector. $\mathcal{D}g(y_1, ..., y_p)$ is $(\partial g/\partial x_1, \ldots, \partial g/\partial x_p)$ evaluated at $(x_1, ..., x_p) = (y_1, ..., y_p)$.

for t in the maximal domain of existence of $\phi^\epsilon(t,x_0)$. Partition $\Phi^\epsilon(t,x_0)$ compatible with $(z_1, z_{2:k}, \eta)$, viz

$$\Phi^\epsilon(t,x_0) = \begin{bmatrix} \Phi^\epsilon_{11}(t,x_0) & \Phi^\epsilon_{12}(t,x_0) & \Phi^\epsilon_{13}(t,x_0) \\ \Phi^\epsilon_{21}(t,x_0) & \Phi^\epsilon_{22}(t,x_0) & \Phi^\epsilon_{23}(t,x_0) \\ \Phi^\epsilon_{31}(t,x_0) & \Phi^\epsilon_{32}(t,x_0) & \Phi^\epsilon_{33}(t,x_0) \end{bmatrix}.$$

Lemma 1: For all $x_0 \in \mathcal{Z}$, the entries of the sensitivity matrix $\Phi^\epsilon(t,x_0)$ satisfy:

i. $\Phi^\epsilon_{31}(t,x_0) = \Phi^\epsilon_{32}(t,x_0) = 0$.
ii. $\Phi^\epsilon_{11}(t,x_0)$, $\Phi^\epsilon_{21}(t,x_0)$, $\Phi^\epsilon_{12}(t,x_0)$, and $\Phi^\epsilon_{22}(t,x_0)$ are independent of ϵ.
iii. $\Phi^\epsilon_{33}(t,x_0) = e^{A(\epsilon)t}$

Proof:

The trajectory sensitivity matrix may be calculated as follows [20]:

$$\begin{Bmatrix} \dot{x} \\ \dot{\Phi} \end{Bmatrix} = \begin{Bmatrix} f^\epsilon(x) \\ \mathcal{D}f^\epsilon(x)\Phi \end{Bmatrix} \text{ with i.c. } \begin{Bmatrix} x_0 \\ I \end{Bmatrix}. \quad (21)$$

Hypothesis H2.1 implies that for $i \in \{1,2,3\}$, $\mathcal{D}_i f^\epsilon_{1:k}(z_1, z_{2:k}, \eta)$ is independent of ϵ and that $\mathcal{D}_1 f^\epsilon_{k+1:n}(z_1, z_{2:k}, \eta) = 0$, $\mathcal{D}_2 f^\epsilon_{k+1:n}(z_1, z_{2:k}, \eta) = 0$, and $\mathcal{D}_3 f^\epsilon_{k+1:n}(z_1, z_{2:k}, \eta) = A(\epsilon)$. By the Peano-Baker formula, the trajectory sensitivity matrix satisfies

$$\begin{aligned} &\Phi^\epsilon(t,x_0) = I + \textstyle\int_0^t K^\epsilon(\tau_1,x_0)\ d\tau_1 + \\ &\textstyle\int_0^t \int_0^{\tau_1} K^\epsilon(\tau_1,x_0)K^\epsilon(\tau_2,x_0)\ d\tau_2 d\tau_1 + \\ &+ \textstyle\int_0^t \int_0^{\tau_1} \int_0^{\tau_2} K^\epsilon(\tau_1,x_0)K^\epsilon(\tau_2,x_0)K^\epsilon(\tau_3,x_0)\ d\tau_3 d\tau_2 d\tau_1 \\ &+ \ \cdots \end{aligned}$$

where, since $x_0 \in \mathcal{Z}$, and $\mathcal{Z}$ is invariant under the solution of $\dot{x} = f^\epsilon(x)$,

$$K^\epsilon(t,x_0) := \mathcal{D}f^\epsilon(x)|_{x=\phi_{\mathcal{Z}}(t,x_0)}. \quad (22)$$

Evaluating the expansion term-by-term then verifies the lemma. ∎

Lemma 2: Let $(z_1^*, z_{2:k}^*, \eta^*) = x^*$ represent the fixed point and $t^* = T_I^\epsilon \circ \hat{\Delta}(z_{2:k}^*, \eta^*)$ be the fundamental period of the periodic orbit $\mathcal{O}$. Then,

$$\mathcal{D}\hat{P}^\epsilon(z_{2:k}^*, \eta^*) = \mathrm{C}(\mathrm{FT} + \mathrm{Q})\mathrm{R}, \quad (23)$$

with matrices $\mathrm{C}, \mathrm{F}, \mathrm{T}, \mathrm{Q}$, and R as defined in (24); moreover, when partitioned compatibly with $(z_1, z_{2:k}, \eta)$, these matrices have the indicated structure[4]:

$$\mathrm{C} := \mathcal{D}\pi(z_1^*, z_{2:k}^*, \eta^*) = \begin{bmatrix} 0 & I & 0 \\ 0 & 0 & I \end{bmatrix} \quad (24a)$$

$$\mathrm{F} := \mathcal{D}_1\phi^\epsilon(t^*, \hat{\Delta}(z_{2:k}^*, \eta^*)) = \begin{bmatrix} \mathrm{F}_1 \\ \mathrm{F}_2 \\ 0 \end{bmatrix} \quad (24b)$$

$$\mathrm{T} := \mathcal{D}T_I^\epsilon(\hat{\Delta}(z_{2:k}^*, \eta^*)) = \begin{bmatrix} \mathrm{T}_1 & \mathrm{T}_2 & \mathrm{T}_3^\epsilon \end{bmatrix} \quad (24c)$$

$$\mathrm{Q} := \Phi^\epsilon(t^*, \hat{\Delta}(z_{2:k}^*, \eta^*)) = \begin{bmatrix} \mathrm{Q}_{11} & \mathrm{Q}_{12} & \mathrm{Q}_{13}^\epsilon \\ \mathrm{Q}_{21} & \mathrm{Q}_{22} & \mathrm{Q}_{23}^\epsilon \\ 0 & 0 & e^{A(\epsilon)t^*} \end{bmatrix} \quad (24d)$$

$$\mathrm{R} := \mathcal{D}\hat{\Delta}(z_{2:k}^*, \eta^*) = \begin{bmatrix} \mathrm{R}_{11} & \mathrm{R}_{12} \\ \mathrm{R}_{21} & \mathrm{R}_{22} \\ 0 & \mathrm{R}_{32} \end{bmatrix}. \quad (24e)$$

Proof:

Equation (23) follows from the chain rule, using

$$\begin{aligned} (z_1^*, z_{2:k}^*, \eta^*) &= \phi^\epsilon(T_I^\epsilon \circ \hat{\Delta}(z_{2:k}^*, \eta^*), \hat{\Delta}(z_{2:k}^*, \eta^*)) \\ &= \phi_{\mathcal{Z}}(T_{I,\mathcal{Z}} \circ \hat{\Delta}(z_{2:k}^*, \eta^*), \hat{\Delta}(z_{2:k}^*, \eta^*)), \end{aligned} \quad (25a)$$

$$\begin{aligned} t^* &= T_I^\epsilon \circ \hat{\Delta}(z_{2:k}^*, \eta^*) \\ &= T_{I,\mathcal{Z}} \circ \hat{\Delta}(z_{2:k}^*, \eta^*), \text{ and} \end{aligned} \quad (25b)$$

$$\Phi^\epsilon(t^*, \hat{\Delta}(z_{2:k}^*, \eta^*)) = \mathcal{D}_2\phi^\epsilon\left(t^*, \hat{\Delta}(z_{2:k}^*, \eta^*)\right). \quad (25c)$$

The structure of C is immediate from the definition of π in (16). From [20, App. D], $F = f^\epsilon(z_1^*, z_{2:k}^*, \eta^*)$, leading to $F_3 = 0$ because $\eta^* = 0$. Also from [20, App. D], T_I^ϵ is differentiable due to the transversality condition H2.5 with

$$\begin{aligned} &\mathcal{D}T_I^\epsilon(\hat{\Delta}(z_{2:k}^*, \eta^*)) = \\ &-(L_{f^\epsilon}H(x^*))^{-1}\left(\tfrac{\partial H}{\partial x}(x^*)\right)^T \Phi^\epsilon(t^*, \hat{\Delta}(z_{2:k}^*, \eta^*)). \end{aligned} \quad (26)$$

The structure of Q is given by Lemma 1, and the form of R follows from H2.2, namely, (8). ∎

Lemma 3: At the fixed point x^*, the linearization of the Poincaré map is

$$\mathcal{D}\hat{P}^\epsilon(z_{2:k}^*, \eta^*) = \begin{bmatrix} M_{11} & M_{12}^\epsilon \\ 0 & M_{22}^\epsilon \end{bmatrix}, \quad (27)$$

and the linearization of the restricted Poincaré map is

$$\mathcal{D}\hat{\rho}(z_{2:k}^*) = M_{11}, \quad (28)$$

where

$$\begin{aligned} M_{11} &= (\mathrm{F}_2\mathrm{T}_1 + \mathrm{Q}_{21})\mathrm{R}_{11} + (\mathrm{F}_2\mathrm{T}_2 + \mathrm{Q}_{22})\mathrm{R}_{21}, \\ M_{12}^\epsilon &= (\mathrm{F}_2\mathrm{T}_1 + \mathrm{Q}_{21})\mathrm{R}_{12} + (\mathrm{F}_2\mathrm{T}_2 + \mathrm{Q}_{22})\mathrm{R}_{22} \\ &\quad + (\mathrm{F}_2\mathrm{T}_3^\epsilon + \mathrm{Q}_{23}^\epsilon)\mathrm{R}_{32}, \text{ and} \\ M_{22}^\epsilon &= e^{A(\epsilon)t^*}\mathrm{R}_{32}. \end{aligned} \quad (29)$$

Proof: Multiplying out (23) and using the structure in (24) proves (27). The second part follows because the Poincaré map leaves $\mathcal{S} \cap \mathcal{Z}$ invariant. In local coordinates, direct calculation yields

$$\begin{aligned} \mathcal{D}\hat{\rho}(z_{2:k}^*) &= \mathcal{D}\pi_2(z_{2:k}^*, \eta^*)\ \mathcal{D}\hat{P}^\epsilon(z_{2:k}^*, \eta^*)\ \mathcal{D}\mathcal{I}(z_{2:k}^*) \\ &= \begin{bmatrix} I & 0 \end{bmatrix} \begin{bmatrix} M_{11} & M_{12}^\epsilon \\ 0 & M_{22}^\epsilon \end{bmatrix} \begin{bmatrix} I \\ 0 \end{bmatrix} \\ &= M_{11}. \end{aligned} \quad (30)$$

∎

[4]For a related decomposition, using a slightly different structure, see [7].

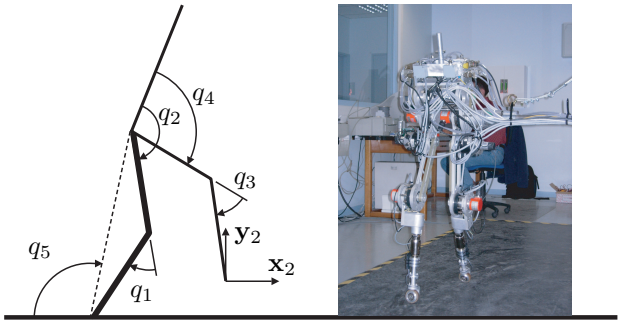

Fig. 3. Coordinate system for the planar bipedal robot RABBIT. The world frame is assumed attached at the base of the stance foot. There are four actuators, two at the knees at two at the hips. The contact point with the ground is unactuated. RABBIT was developed as part of the French National Project, ROBEA, and is housed at LAG (Grenoble) [21]. Eric Westervelt is in the background.

C. Proof of Theorem 2

Suppose that x^* is an exponentially stable fixed point of ρ. Then by (28), the eigenvalues of M_{11} have magnitude less than one. By H2.6 and (29), $\lim_{\epsilon \searrow 0} M_{22}^{\epsilon} = \lim_{\epsilon \searrow 0} e^{A(\epsilon)t^*} \mathrm{R}_{32} = 0$, and therefore, because eigenvalues depend continuously on the entries of the matrix, there exists $\bar{\epsilon} > 0$ such that for $0 < \epsilon < \bar{\epsilon}$, the eigenvalues of M_{22}^{ϵ} all have magnitude less than one, and hence, x^* is an exponentially stable fixed point of P^{ϵ}.

The other direction is trivial.

V. Application to a Bipedal Robot

This section studies the exponential stability of a periodic walking motion in an underactuated, planar bipedal robot; see Fig. 3-(b). The model is naturally represented as a system with impulse effects. Prior to the result of Section III, stability of a walking gait was analyzed with a result proven in [11] that differed from Theorem 2 in two respects: (a) it required that the surface $\mathcal{Z}$ be invariant under the differential equation part of the system with impulse effects and *finite-time attractive* (the latter property was achieved with a continuous, but not Lipschitz-continuous feedback control law [3], [2]); (b) the result did not require that $\mathcal{Z}$ be invariant under the impact map. However, after [11], feedback designs that systematically create $\mathcal{Z}$ so as to be invariant under the impact map have been presented in [24], [5], [12], [6], for example. The objective of this section is to show that by exploiting this additional invariance property, namely, $\Delta(\mathcal{S} \cap \mathcal{Z}) \subset \mathcal{Z}$, exponentially stable walking gaits can be created with a smooth feedback controller.

A. Open-loop model

A model of RABBIT with coordinates $q = (q_1, \ldots, q_5) \in \mathcal{Q}$ as shown in Fig. 3-(a) is briefly summarized. Following [5], the method of Lagrange leads to the standard mechanical model

$$D(q)\ddot{q} + C(q,\dot{q})\dot{q} + G(q) = Bu, \text{ with } B = \begin{bmatrix} I \\ 0 \end{bmatrix}. \quad (31)$$

	Femur	Tibia	Torso
Length (m)	0.4	0.4	0.625
Mass (kg)	6.8	3.2	17.0
Inertia (kg-m^2)	0.47	0.20	1.33

TABLE I
Experimentally measured parameters for RABBIT.

The impact (i.e., switching) surface is $\mathcal{S} = \{(q,\dot{q}) \in T\mathcal{Q} \mid \mathbf{y}_2(q) = 0,\ \mathbf{x}_2(q) > 0\}$, the set of points where the swing leg height is zero and in front of the stance leg. When the swing leg contacts the ground, an inelastic impact is assumed, giving rise to a jump in the velocity coordinates[5]. An impact map $\Delta : \mathcal{S} \to T\mathcal{Q}$ can be computed as in [15], [11], [5]. Defining $x := (q;\dot{q})$, the mechanical model is expressed in state variable form as a controlled system with impulse effects:

$$\Sigma_{\mathrm{ol}} : \begin{cases} \dot{x} = & f_{ol}(x) + g(x)u & x^- \notin \mathcal{S} \\ x^+ = & \Delta(x^-) & x^- \in \mathcal{S}, \end{cases} \quad (32)$$

where the vector of control torques is $u \in I\!R^4$.

B. Feedback controller

The feedback designs developed in [24] are based on virtual constraints, which are holonomic constraints on the robot's configuration that are asymptotically imposed through feedback control. Their function is to coordinate the evolution of the various links throughout a step. Since RABBIT has four independent actuators (two at the hips and two and the knees), four virtual constraints may be imposed. Following [24], since q_5 is naturally monotonic as the robot advances from left to right in a step, the four virtual constraints are written as

$$y = h(q) := q_b - h_d(q_5), \quad (33)$$

where $q_b = (q_1, \ldots, q_4)$ is the vector of actuated (body) coordinates, and $h_d(q_5)$ gives the desired configuration of the actuated joints as the robot advances in a step. Here, h_d is chosen as in the example in [24, Sect. VII].

Because $y = h(q)$ depends only on the configuration variables, its relative degree is at least two. Differentiating the output twice gives

$$\ddot{y} = L_f^2 h(q,\dot{q}) + L_g L_f h(q) u. \quad (34)$$

Suppose for the moment that the decoupling matrix $L_g L_f h$ is invertible. Let $K_D = k_D I_{4\times 4}$ and $K_P = k_P I_{4\times 4}$, where

$$\lambda^2 + k_D \lambda + k_P = 0 \quad (35)$$

[5]So that the same mechanical model can be used independent of which leg is the stance leg, the coordinates must also be relabeled, giving rise to a jump in the configuration variables as well; see[11], [24], [5]. The impact map satisfies $\Delta(\mathcal{S}) \cap \mathcal{S} = \emptyset$.

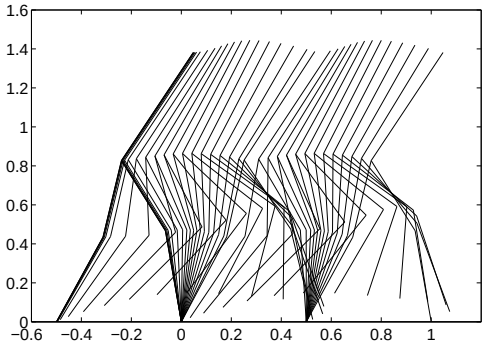

Fig. 4. A stick-figure animation of the walking motion used in the example.

has distinct roots with negative real parts, and let $\epsilon > 0$. Then the feedback law

$$u(x) = -\left(L_g L_f h(x)\right)^{-1}\Big(L_f^2 h(x) + \frac{1}{\epsilon} K_D L_f h(x) + \frac{1}{\epsilon^2} K_P h(x)\Big) \tag{36}$$

applied to $\dot{x} = f_{ol}(x) + g(x)u$ results in [16]

$$\ddot{y} = -\frac{1}{\epsilon} K_D \dot{y} - \frac{1}{\epsilon^2} K_P y. \tag{37}$$

Moreover,

$$\mathcal{Z} := \{x \in T\mathcal{Q} \mid h(x) = 0,\ L_f h(x) = 0\}$$

is a smooth two-dimensional submanifold of $T\mathcal{Q}$ and is invariant under the closed-loop dynamics

$$f^\epsilon(x) := f_{ol}(x) + g(x)u(x).$$

In [24, Sect. V-VII], it is shown how to design h_d using Bézier polynomials and sequential numerical optimization so that the decoupling matrix $L_g L_f h$ is invertible, $\Delta(\mathcal{S} \cap \mathcal{Z}) \subset \mathcal{Z}$, the restricted Poincaré map has an exponentially stable fixed point, and the orbit is transversal to $\mathcal{S} \cap \mathcal{Z}$, while meeting other performance objectives involving walking speed, actuator power, and the contact forces at the leg ends. Since RABBIT has five degrees of freedom in the stance phase and four independent actuators, the restricted Poincaré map is scalar valued, and hence M_{11} in (29) is a scalar. For the choice of virtual constraints used here (i.e., h_d), $M_{11} = 0.58$; a stick-figure animation of the walking motion is shown in Fig. 4.

C. Closed-loop analysis

The objective is to understand when the exponentially stable orbit in $\mathcal{Z}$ is also exponentially stable in the full-order model (32) with feedback law (36). Based on Theorem 2 and Lemma 3, the objective is to put f^ϵ in the proper coordinates so that the Hypotheses H2 can be checked. Note that because $h(q) = q_b - h_d(q_5)$,

$$\Psi(q) = \begin{bmatrix} h(q) \\ q_5 \end{bmatrix} \tag{38}$$

is a global diffeomorphism on $\mathcal{Q}$. It follows that

$$\begin{bmatrix} z_1 \\ z_2 \\ \eta_{1:4} \\ \eta_{5:8} \end{bmatrix} = \begin{bmatrix} q_5 \\ D_5(q)\dot{q} \\ h(q) \\ \frac{\partial h}{\partial q}(q)\dot{q} \end{bmatrix} \tag{39}$$

is a global diffeomorphism on $T\mathcal{Q}$, where D_5 is the last row of D in (31) and $\sigma := D_5(q)\dot{q}$ is the angular momentum of the biped about the end of the stance leg [5]. In these coordinates [16, pp. 224],

$$f^\epsilon(z,\eta) = \begin{bmatrix} f_{1:2}(z,\eta) \\ A(\epsilon)\eta \end{bmatrix}, \tag{40}$$

where

$$A(\epsilon) = \begin{bmatrix} 0 & I_{4\times 4} \\ \frac{-k_P}{\epsilon^2} I_{4\times 4} & \frac{-k_D}{\epsilon} I_{4\times 4} \end{bmatrix}. \tag{41}$$

To verify $\lim_{\epsilon \searrow 0} e^{A(\epsilon)} = 0$ as required in H2.6, note that

$$A(\epsilon) = \Pi(\epsilon)\frac{1}{\epsilon} A_0 \Pi^{-1}(\epsilon), \tag{42}$$

where

$$A_0 = \begin{bmatrix} 0 & I_{4\times 4} \\ -k_P I_{4\times 4} & -k_D I_{4\times 4} \end{bmatrix} \tag{43}$$

and

$$\Pi(\epsilon) = \begin{bmatrix} \epsilon I_{4\times 4} & 0 \\ 0 & I_{4\times 4} \end{bmatrix}. \tag{44}$$

Since (35) is a Hurwitz polynomial, $e^{\frac{1}{\epsilon}A_0}$ goes to zero exponentially fast as $\epsilon \to 0$, and hence $\lim_{\epsilon \searrow 0} e^{A(\epsilon)} = 0$.

In conclusion, for $\epsilon > 0$ sufficiently small, the feedback law (36) exponentially stabilizes in the full-order model a periodic orbit that is exponentially stable in the restriction dynamics. This is investigated numerically in the next subsection.

D. Simulation: walking on flat ground

The eigenvalues of $\mathcal{D}P^\epsilon$ were computed at the fixed point for various values of $\epsilon > 0$. Table II shows that the eigenvalue associated with the restricted Poincaré map (shown in bold) is indeed constant for varying values of ϵ. This table indicates that for $\epsilon \leq 0.17$, the periodic motion is exponentially stable in the full-order model, but for $\epsilon = 0.20$, it is unstable. Note that due to the impact map, $\mathcal{D}P^\epsilon$ may have negative real eigenvalues; see (29).

Figure 5 shows that decreasing ϵ causes $\|\eta(t)\|_2$ to converge to zero more quickly. Discontinuities in $\eta(t)$ occur at each impact event, with the impact tending to increase $\|\eta(t)\|_2$ rather than decrease it. From Lemma 3 and (41), it follows that $\log(\det(\mathcal{D}P^\epsilon))$ should be affine in $1/\epsilon$. This is confirmed in Fig. 6, lending credibility to the numerical computations.

TABLE II

EIGENVALUES OF $\mathcal{D}P^\epsilon$ FOR THREE VALUES OF ϵ, RANKED BY MAGNITUDE. THE EIGENVALUE OF $\mathcal{D}\rho$ IS SHOWN IN BOLD.

$\epsilon = 0.12$	$\epsilon = 0.17$	$\epsilon = 0.20$
0.58	-0.62	$\boxed{-1.91}$
0.48	**0.58**	**0.58**
$-0.12 + 4.4 \times 10^{-2}\ i$	$-0.19 + 0.14\ i$	$-0.12 + 0.27\ i$
$-0.12 - 4.4 \times 10^{-2}\ i$	$-0.19 - 0.14\ i$	$-0.12 + 0.27\ i$
$-0.11 - 5.4 \times 10^{-2}\ i$	$-0.17 + 0.16\ i$	$-0.15 + 0.25\ i$
$-0.11 + 5.4 \times 10^{-2}\ i$	$-0.17 - 0.16\ i$	$-0.15 + 0.25\ i$
2.5×10^2	0.14	0.21
$9.2 \times 10^{-3} - 1.8 \times 10^{-2}\ i$	-8.2×10^{-2}	-4.2×10^{-2}
$9.2 \times 10^{-3} + 1.8 \times 10^{-2}\ i$	8.0×10^{-3}	7.6×10^{-3}

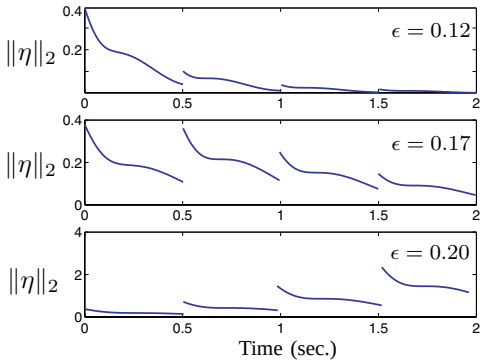

Fig. 5. Evolution of $\|\eta(t)\|_2$ for three values of ϵ. The restricted system corresponds to $\eta \equiv 0$. As ϵ decreases to zero, $\eta(t)$ converges more quickly to zero. Note that the orbit is unstable for $\epsilon = 0.2$ even though it is exponentially stable in the restricted dynamics and the "transversal part" of the closed-loop ODE is decoupled, linear, and exponentially stable.

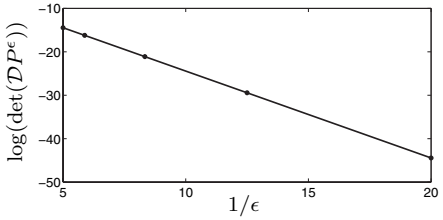

Fig. 6. The graph of $\log(\det(\mathcal{D}P^\epsilon))$ versus $1/\epsilon$ should be affine when the controller (36) is used.

VI. CONCLUSION

This paper has established conditions under which a periodic orbit in a system with impulse effects is exponentially stable, if, and only if, the orbit is exponentially stable in a hybrid restriction dynamics. In a case study, the utility of this result was highlighted: a periodic orbit whose design was carried out on the basis of a two-dimensional restriction dynamics (i.e., the hybrid zero dynamics of walking) could be systematically rendered exponentially stable in the full-order model by using a smooth state-variable feedback. The improvement over previous work is that finite-time attractivity of an invariant surface could be replaced by sufficiently fast exponential attractivity, and a wider class of feedback control laws can be applied.

There are numerous ways to extend the basic result. For example the transversal dynamics do not need to be linear, and the Hypotheses H2 can be stated in more geometric terms.

REFERENCES

[1] D. Bainov and P. Simeonov, *Systems with Impulse Effects : Stability, Theory and Applications*. Chichester: Ellis Horwood Limited, 1989.

[2] S. Bhat and D. Bernstein, "Continuous finite-time stabilization of the translational and rotational double integrators," *IEEE Transactions on Automatic Control*, vol. 43, no. 5, pp. 678–682, 1998.

[3] ——, "Finite-time stability of continuous autonomous systems," *SIAM Journal of Control and Optimization*, vol. 38, no. 3, pp. 51–766, 2000.

[4] V. Chellaboina, S. P. Bhat, and W. M. Haddad, "An invariance principle for nonlinear hybrid and impulsive dynamical systems," *Nonlinear Analysis*, vol. 53, pp. 527–50, 2003.

[5] C. Chevallereau, G. Abba, Y. Aoustin, E. Plestan, F. Westervelt, C. Canudas-de Wit, and J. Grizzle, "RABBIT: A testbed for advanced control theory," *IEEE Control Systems Magazine*, vol. 23, no. 5, pp. 57–79, October 2003.

[6] J. Choi and J. Grizzle, "Planar bipedal robot with impulsive foot action," in *IEEE Conf. on Decision and Control*, 2004.

[7] M. Colemen, A. Chatterjee, and A. Ruina, "Motions of a rimless spoked wheel: a simple 3d system with impacts," in *Dynamics and Stability of Systems*, vol. 12, no. 3, 1997, pp. 139–160.

[8] S. Collins, M. Wisse, and A. Ruina, "A three-dimensional passive-dynamic walking robot with two legs and knees," *International Journal of Robotics Research*, vol. 20, no. 7, pp. 607–615, July 2001.

[9] J. Goncalves, A. Megretski, and M. Dahleh, "Global stability of relay feedback systems," *TAC*, vol. 46, no. 4, pp. 550 – 562, April 2001.

[10] A. Goswami, B. Espiau, and A. Keramane, "Limit cycles and their stability in a passive bipedal gait," in *Proc. of the IEEE International Conference on Robotics and Automation, Minneapolis, MN.*, April 1996, pp. 246–251.

[11] J. Grizzle, G. Abba, and F. Plestan, "Asymptotically stable walking for biped robots: Analysis via systems with impulse effects," *IEEE Transactions on Automatic Control*, vol. 46, pp. 51–64, January 2001.

[12] J. Grizzle, E. Westervelt, and C. Canudas-de-Wit, "Event-based PI control of an underactuated biped walker," in *IEEE Conf. on Decision and Control*. IEEE Press, December 2003.

[13] J. Guckenheimer and P. Holmes, *Nonlinear Oscillations, Dynamical Systems, and Bifurcations of Vector Fields*, corrected second printing ed., ser. Applied Mathematical Sciences. New York: Springer-Verlag, 1996, vol. 42.

[14] I. Hiskens, "Stability of hybrid limit cycles: application to the compass gait biped robot," in *Proc. of the 40th IEEE Conf. Dec. and Control, Orlando, FL*, December 2001, pp. 774–779.

[15] Y. Hurmuzlu and D. Marghitu, "Rigid body collisions of planar kinematic chains with multiple contact points," *International Journal of Robotics Research*, vol. 13, no. 1, pp. 82–92, 1994.

[16] A. Isidori, *Nonlinear Control Systems: An Introduction*, 3rd ed. Berlin: Springer-Verlag, 1995.

[17] H. Khalil, *Nonlinear Systems - 2nd Edition*. Upper Saddle River: Prentice Hall, 1996.

[18] A. Kuo, "Stabilization of lateral motion in passive dynamic walking," *International Journal of Robotics Research*, vol. 18, no. 9, pp. 917–930, 1999.

[19] S. Nersesov, V. Chellaboina, and W. Haddad, "A generalization of Poincaré's theorem to hybrid and impulsive dynamical systems," *Int. J. Hybrid Systems*, vol. 2, pp. 35–51, 2002.

[20] T. Parker and L. Chua, *Practical Numerical Algorithms for Chaotic Systems*. New York: Springer-Verlag, 1989.

[21] ROBEA: Robotics and Artificial Entities, "robot-rabbit.lag.ensieg.inpg.fr/index.php (in French; for an English version, click on the British flag)," March 2005.

[22] A. V. Roup, D. S. Bernstein, S. G. Nersesov, W. M. Haddad, and V. Chellaboina, "Limit cycle analysis of the verge and foliot clock escapement using impulsive differential equations and Poincare maps," *Int. J. Control*, vol. 76, no. 17, pp. 1685–1698, 2003.

[23] B. Thuilot, A. Goswami, and B. Espiau, "Bifurcation and chaos in a simple passive bipedal gait," in *Proc. of the IEEE International Conference on Robotics and Automation, Albuquerque, N.M.*, April 1997, pp. 792–798.

[24] E. Westervelt, J. Grizzle, and D. Koditschek, "Hybrid zero dynamics of planar biped walkers," *IEEE Transactions on Automatic Control*, vol. 48, no. 1, pp. 42–56, January 2003.

[25] H. Ye, A. Michel, and L. Hou, "Stability theory for hybrid dynamical systems," *IEEE Transactions on Automatic Control*, vol. 43, no. 4, pp. 461–474, April 1998.